EXIT Chart-Aided Adaptive Coding for MMSE Turbo Equalization with Multilevel BICM

Shinsuke Ibi, *Student Member, IEEE,* Tad Matsumoto, *Senior Member, IEEE,* Seiichi Sampei, *Senior Member, IEEE,* and Norihiko Morinaga, *Fellow, IEEE*

***Abstract*— This letter proposes adaptive coding (AC) for multi-level bit interleaved coded modulation (ML-BICM) with MMSE turbo equalization, of which aim is to minimize the information rate loss due to the mismatch between the channel realization and channel coding. With the aid of the knowledge about extrinsic information transfer (EXIT) characteristics at the receiver, the code parameters such as code rates and/or generator polynomials are adaptively selected independently in each the ML-BICM layer. Numerical results show that throughput efficiency can be significantly improved with the proposed AC technique over the automatic repeat request (ARQ) technique with fixed code rate.**

***Index Terms*— Turbo equalization, soft interference cancellation, frequency domain MMSE equalization, EXIT analysis, adaptive coding.**

I. INTRODUCTION

MMSE turbo equalization has been recognized as one of the most promising techniques for broadband mobile communication applications using single-carrier signaling [1], [2]. Reference [3] extends the MMSE turbo equalization to bit interleaved coded modulation (BICM) using higher-order modulation such as quadrature amplitude modulation (QAM), constructed with arbitrary mapping rules. Reference [4] uses a different technique, where the QAM constellation is constructed by linearly weighted multiple *binary* sequences, for which this technique is referred to as multi-level (ML)-BICM. A beneficial point of the ML-BICM approach is that the equalizer can separate the binary sequences constituting the QAM layers. In fact, Ref. [4] utilizes the benefit of the cross-layer separability in automatic repeat request (ARQ) where re-transmission control takes place independently in each the layer. With this technique, much higher throughput efficiency, as a whole, can be achieved over BICM with single ARQ. Despite the throughput merit achieved by ML-BICM with stream-wise ARQ, there is still a mismatch between the given channel realization and the coding scheme used by the each stream, resulting in two detrimental situations: One is the case where turbo equalization does not converge, and the other where the code redundancy is too high to maintain the information rate inherently achievable by the channel itself.

Manuscript received November 26, 2005. The associate editor coordinating the review of this letter and approving it for publication was Prof. Jing Li.

S. Ibi and S. Sampei are with the Graduate School of Engineering, Osaka University, 2-1 Yamada-oka, Suita, Osaka 565-0871, Japan (e-mail: ibi@wireless.comm.eng.osaka-u.ac.jp, sampei@comm.eng.osaka-u.ac.jp).

T. Matsumoto is with the Centre for Wireless Communications, University of Oulu, Erkki Koiso-Kanttilan katu 3, Oulu 90570, Finland (e-mail: tadashi.matsumoto@ee.oulu.fi).

N. Morinaga is with the Dept. of Information Technology, Hiroshima International University, 5-1-1 hiro-koshingai, Kure, Hiroshima 737-0112, Japan (e-mail: morinaga@it.hirokoku-u.ac.jp).

Digital Object Identifier 10.1109/LCOMM.2006.06003.

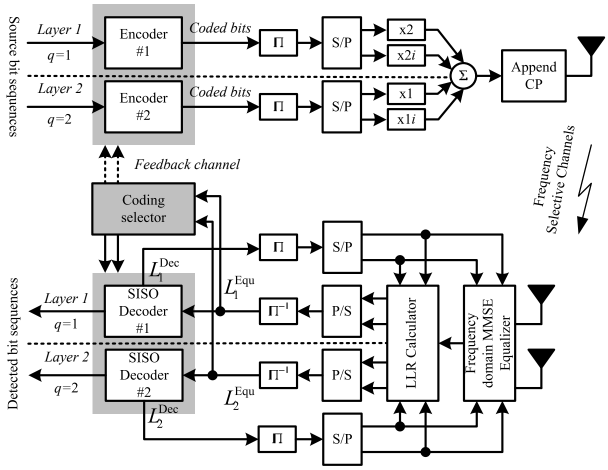

Fig. 1. Block diagram of the considered system (16QAM: $M = 4$).

The focus point in this letter is on adaptive coding (AC) for ML-BICM with MMSE turbo equalization, of which aim is to minimize the information rate loss due to the mismatch. With the aid of the knowledge about extrinsic information transfer (EXIT) characteristics [5], the code parameters such as code rates and/or generator polynomials are adaptively selected independently in the each QAM layer, so that the information rate loss is minimized.

After the brief explanation of the system model in Section II, this letter describes the proposed AC technique for ML-BICM MMSE turbo equalization in Section III. Section IV presents numerical results to demonstrate the throughput enhancement achieved by the proposed AC technique.

II. CONSIDERED SYSTEM

A block diagram of the system considered in this letter is shown in Fig. 1, where 16 QAM is assumed as an example. In ML-BICM, signals to be transmitted are constructed from $M/2$ independent binary coded sequences that are linearly weighted and summed up to construct 2^M QAM constellation points. There are $M/2$ layers, each having the same amplitude. Each of the $M/2$ binary sequences are encoded by their encoders selected by the receiver from among the available code set, and the selected codes are notified via the feedback channel. The coded sequences, each having $2K$ symbols, are interleaved and serial-to-parallel converted into two length K

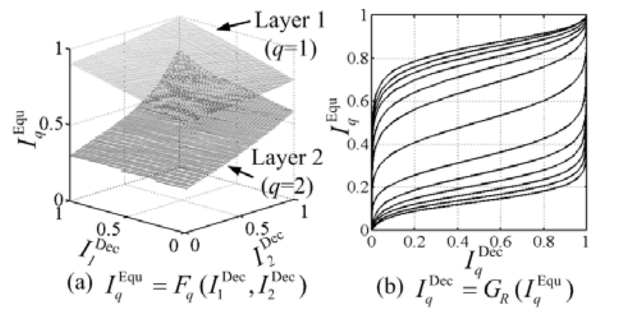

Fig. 2. Extrinsic information transfer characteristics of (a) equalizer and (b) decoders: (a) example snapshot of $L = 10$ and instantaneous $E_s/N_0 = 8$ dB, (b) coding rates R =7/8, 6/7, 5/6, 4/5, 3/4, 2/3, 1/2, 1/3, 1/4, 1/5, 1/6, 1/7, and 1/8 with constraint length 3 from top to bottom.

bit-streams to be transmitted over the inphase- and quadrature-channels, respectively, of the corresponding layer. The M streams for the all layers are then mapped on to 2^M QAM constellation points, according to the linear mapping rule described in Introduction. A length P-symbol cyclic prefix is appended to the head of the frame to be transmitted, allowing for frequency domain processing at the receiver, resulting in $K + P$ symbols in each frame.

The transmitted signal propagates over L-path frequency-selective fading channels, and received by a receiver having N_R antennas. It is assumed that the channels remain static over each transmitted frame. At the receiver, turbo equalization using soft cancellation and frequency domain MMSE filtering is used to mitigate inter-symbol interference (ISI). The derivation of the equalization algorithm is detailed in Ref. [6]. Even though we assume ML-BICM, the MMSE turbo equalizer first calculates the symbol-wise log likelihood ratio (LLR) for the linear mapping used by ML-BICM, and then convert it into a set of bit-wise LLRs for the each layer. The derivation of the bit-wise LLR follows Ref. [3]. The extrinsic LLR for the q-th layer is propagated between the equalizer and the decoder, of which flows are denoted by $L_q^{\mathrm{Dec}} \to L_q^{\mathrm{Equ}}$ and $L_q^{\mathrm{Equ}} \to L_q^{\mathrm{Dec}}$, respectively, via deinterleaver and interleaver.

III. Adaptive Coding Scheme

A. EXIT Properties for ML-BICM

The mutual information (MI) I between the coded bits $\mathcal{S} \in \pm 1$ with equiprobable occurrence and the LLR L is given by [5]

$$I = 1 - \int_{-\infty}^{\infty} p_{L|\mathcal{S}}(\xi| + 1) \log_2 \left(1 + e^{-\xi}\right) d\xi \qquad (1)$$

where $p_{L|\mathcal{S}}(\xi|b)$ is the probability density function (PDF) of LLR being ξ conditioned upon the coded bit b.

The EXIT charts for the equalizer and the decoders are depicted in Figs. 2 (a) and (b), respectively, for the parameter described in the figure caption. In 2 (a), the symbol energy-to-noise density ratio (E_s/N_0) is set at 8 dB. MI for the equalizer and decoder, I_q^{Equ} and I_q^{Dec}, are calculated by substituting the measured LLR histograms, given L_q^{Equ} and L_q^{Dec}, into Eq. (1). The equalizer MI transfer characteristics are expressed by *planes* since the MI depends on the feedback MI from each layer's decoder, as

$$I_q^{\mathrm{Equ}} = F_q(I_1^{\mathrm{Dec}}, I_2^{\mathrm{Dec}}), \quad (q = 1, 2 \text{ for 16QAM}). \qquad (2)$$

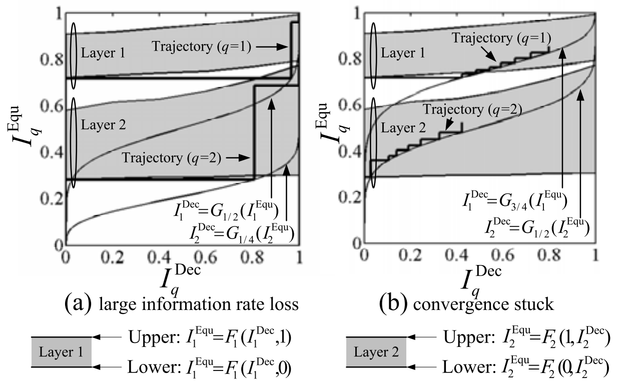

Fig. 3. Snapshots of trajectories in iterative decoding: (a) codes with R = 1/2 and 1/4 are used for layer 1 and 2, respectively (b) codes with R = 3/4 and 1/2 are used for layer 1 and 2, respectively.

As seen in the figure, the EXIT *planes* corresponding to the layers 1 and 2 are separated with each other because ML-BICM constructed with linearly weighted coded sequences. In fact, the *planes* vary depending on the channel realization, which suggests that different codes should be used in the each layer.

Fig. 2 (b) shows the MI transfer characteristics of the channel decoders for the constraint length 4 convolutional codes [7] having rates described in the figure caption. Their MI transfer characteristic is denoted as

$$I_q^{\mathrm{Dec}} = G_R(I_q^{\mathrm{Equ}}). \qquad (3)$$

In order to examine the convergence property, the both equalizer and decoder's MI transfer characteristics are plotted in Figs. 3 (a) and (b). The figures show examples of the trajectory until the eighth iteration. Note that equalizer *planes* shown in Fig. 2 (a) are depicted by projection, so that the lower-bound $F_1(I_1^{\mathrm{Dec}}, 0)$ and the upper-bound $F_1(I_1^{\mathrm{Dec}}, 1)$ are shown instead of the *plane* for layer 1, similarly, $F_2(0, I_2^{\mathrm{Dec}})$ and $F_1(1, I_2^{\mathrm{Dec}})$ for layer 2. Figure 3 (a) is for the case where higher decoder MI can be achieved even at the first iteration, where the information rate loss is incurred, and by using a higher code rate, such rate loss may be reduced. In contrast, Fig. 3 (b) shows the case where convergence is stuck, resulting in high frame error rate (FER).

B. Adaptive Coding Using EXIT Chart

To minimize the rate loss due to the code-equalizer mismatch, given the channel realization, the optimal codes for the each layer of ML-BICM can be found based on the rate-capacity property analysis [8]. However, in practice, this is not feasible because finding EXIT plane requires heavy computational burden, and the planes vary according to the channel variations. Therefore, adjusting the code parameters in real-time such that the code optimality is always exactly guaranteed is not practical.

Now recall the trajectory plots shown in Fig. 3(a). The trajectory in each layer is not affected by the other layer, if the both layers converge. This suggests that code rate may be determined only by examining the point where the equalizer MI curve crosses the decoder MI curve. For convenience, this point is refereed to as T_q^{end} ($q = 1, 2$, for 16QAM). The code having a rate $R_q^{\max}$ is then selected such that

$$R_q^{\max} = \max_{R} \left\{ \gamma_R^{\alpha} < T_q^{\text{end}} \right\}, \tag{4}$$

where γ_R^{α} denotes the required decoder input MI yielding FER $\leq \alpha$ with α being a system design parameter. Note that γ_R^{α} is uniquely determined by the decoder input, and although the bit error ratio can be estimated from decoder output MI, FER depends on the code length. Therefore, the required decoder input MI γ_R^{α} for FER $\leq \alpha$ has to be pre-calculated for the specific parameter of each code in the set through simulations as shown in Sec. IV. Note further that, the MI exchange is stuck even though the criterion Eq. (4) is satisfied. The event is counted as frame error in the numerical evaluation presented in Sec. IV.

C. Empirical Method for Mutual Information Calculation

In order to exactly calculate the MI, perfect knowledge about transmitted bits sequence is needed when evaluating histograms $p_{L|\mathcal{S}}(\xi|b)$. However, in practice, MI has to be calculated without having to know the transmitted coded sequence at the receiver side. Applying Bayes' theorem $p_{L|\mathcal{S}}(\xi|b)p = 2p_L(\xi)p_{\mathcal{S}|L}(b|\xi)$ to Eq. (1), the MI is rewritten as

$$\begin{aligned} I &= 1 - 2\int_{-\infty}^{\infty} p_L(\xi)p_{\mathcal{S}|L}(+1|\xi)\log_2\left(1+e^{-\xi}\right)d\xi \\ &= 1 - 2\mathbb{E}\left\{p_{\mathcal{S}|L}(+1|\xi)\log_2\left(1+e^{-\xi}\right)\right\} \end{aligned} \tag{5}$$

where $\mathbb{E}\{\cdot\}$ denotes expectation, $p_L(\xi)$ is obtained by the LLR histogram measurement, and $p_{\mathcal{S}|L}(b|\xi)$ is approximated by

$$p_{\mathcal{S}|L}(+1|\xi) \approx \left[1+e^{-\xi}\right]^{-1}. \tag{6}$$

Note that the approximation may deteriorate the LLR accuracy in the presence of inferior soft output LLRs such as that obtained by the Max Log-MAP algorithm. Furthermore, by invoking the ergodicity, the expectation can be replaced by time average as

$$I = 1 - \frac{2}{K}\sum_{k=1}^{K}\frac{\log_2\left(1+e^{-L_k}\right)}{1+e^{-L_k}} \tag{7}$$

where L_k is the LLR of the k-th bit in the burst.

IV. Numerical Results and Remarks

Results of the numerical calculations conducted to verify the throughput efficiency enhancement with the AC technique is presented in this section. Spatially uncorrelated two receive antennas were assumed ($N_R = 2$). A ten-path ($L = 10$) channel having equal average power delay profile was assumed for each of the transmitter-receiver antenna pairs. Perfect knowledge about the channels was assumed available at the receiver. To make Eq. (6)'s approximation accurate, the Max-Log-MAP algorithm with a correcting factor proposed by [9] was used in the each layer's SISO decoder. K=2048 and P=64 were assumed.

Throughput efficiencies with selective-repeat ARQ [4] and this letter's proposed AC scheme, both with 16QAM ML-BICM MMSE turbo equalization, are shown in Fig. 4 (a) and (b), respectively. In AC, the FER requirement was set

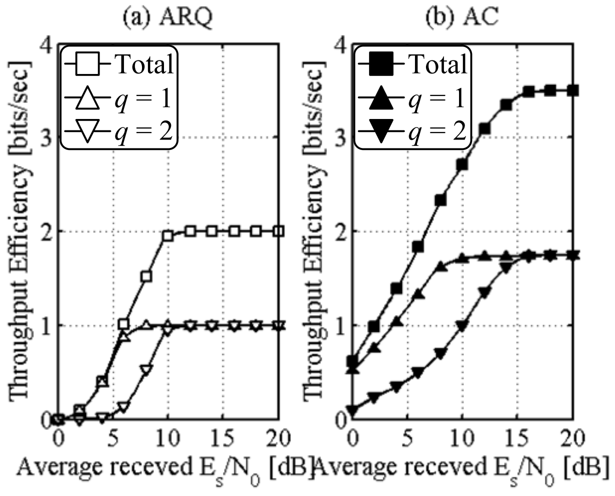

Fig. 4. Throughput efficiencies of (a) ARQ and (b) AC: (a) only constraint length 3 half-rate codes are used for each layer, (b) available code set is described in the caption of Fig. 2 (b).

at $\alpha = 0.1$. The throughput efficiency for the q-th layer was defined as [*summation of number of source bits in successful received frames*]/[*number of received symbols*] for $q = 1$ and 2. The AC's throughput efficiency totaling the layers 1 and 2 is much higher than with ARQ; With ARQ, the Layer-2 does not make any contribution to the total throughput when average $E_s/N_0 \leq 5$ dB; This is because the code rate is fixed. In contrast, the AC allows the both layers to adaptively adjust the code rate, depending on channel realizations. When average E_s/N_0 is large enough, the total throughput plateaus at the sum of the code rates allocated for the both layers for both AC and ARQ. However, AC achieves much higher throughput because it uses higher rate code, whereas it is fixed with ARQ. If higher order modulation is used, the throughput plateau shall be increased with AC.

References

[1] D. Reynolds and X. Wang, "Low complexity turbo-equalization for diversity channels," *Signal Processing, Elsevier Science Publishers*, vol. 81, no. 5, pp. 989–995, May 2001.

[2] T. Abe and T. Matsumoto, "Space-time turbo equalization in frequency-selective MIMO channels," *IEEE Trans. Veh. Technol.*, vol. 52, no. 3, pp. 469–475, May 2003.

[3] A. Dejonghe and L. Vadendorpe, "Turbo-equalization for multilevel modulation: an effcient low-complexity scheme," in *Proc. ICC 2002*, vol. 3, New York, USA, Apr. 28-May 2 2002, pp. 1863–1867.

[4] K. Kansanen, C. Schneider, T. Matsumoto, and R. Thoma, "Multilevel coded QAM with MIMO turbo-equalization in broadband single-carrier signaling," *IEEE Trans. Veh. Technol.*, vol. 54, no. 3, pp. 954–966, May 2005.

[5] S. ten Brink, "Convergence behavior of iteratively decoded parallel concatenated codes," *IEEE Trans. Commun.*, vol. 49, no. 10, pp. 1727–1737, Oct. 2001.

[6] K. Kansanen and T. Matsumoto, "Frequency-domain MMSE turbo equalization – convergence in fading channels," *submitted to IEEE Trans. Wireless Commun.*

[7] J. G. Proakis, *Digital Communications*, 4th ed. New York: McGraw-Hill, 2001.

[8] J. Hagenauer, "The EXIT chart - introduction to extrinsic information transfer in iterative processing," in *Proceedings of 12th European Signal Processing Conferrence (EUSIPCO)*, Sept. 2004, pp. 1541–1548.

[9] P. Robertson, E. Villebrun, and P. Hoeher, "A comparison of optimal and sub-optimal MAP decoding algorithms operating in the log domain," in *'95*, Seattle, USA, June 1995, pp. 1009–1013.